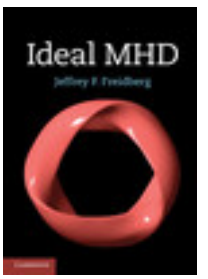

Ideal MHD

Jeffrey P. Freidberg

Book DOI: http://dx.doi.org/10.1017/CBO9780511795046

Online ISBN: 9780511795046

Hardback ISBN: 9781107006256

Chapter

5 - Equilibrium: one-dimensional configurations pp. 85-122

Chapter DOI: http://dx.doi.org/10.1017/CBO9780511795046.006

Cambridge University Press

5

Equilibrium: one-dimensional configurations

5.1 Introduction

Although the magnetic configurations of fusion interest are toroidal, one can begin to develop physical intuition by first investigating their one-dimensional cylindrically symmetric analogs: the θ-pinch, the Z-pinch, and the general screw pinch. These can be considered to be the basic building blocks of MHD equilibrium. Focusing on cylindrical systems allows the two basic problems of MHD equilibrium – radial pressure balance and toroidal force balance – to be separated, so that each can be studied individually.

The one-dimensional model focuses entirely on radial pressure balance. The question of toroidal force balance does not enter since by definition the geometry is a linear cylinder. For many configurations, once radial pressure balance is established, toroidicity can be introduced by means of an inverse aspect ratio expansion, from which one can then investigate toroidal force balance.

Chapter 5 provides a description of the basic one-dimensional configurations and how they provide radial pressure balance in a plasma. In particular, it is shown that both toroidal and poloidal fields as well as combinations thereof can easily accomplish this goal.

Included in the analysis are descriptions of two present day fusion concepts: the reversed field pinch, and the ohmic tokamak. These configurations are singled out since both their radial pressure balance and MHD stability are reasonably well described by the one-dimensional cylindrical model. Toroidal effects can be treated perturbatively and make small quantitative, but not qualitative, corrections to the cylindrical equilibrium and stability results.

5.2 The θ-pinch

The θ-pinch represents the one-dimensional analog of the toroidal configuration with purely toroidal field. The "equivalent" torus consists of a section $2\pi R_0$

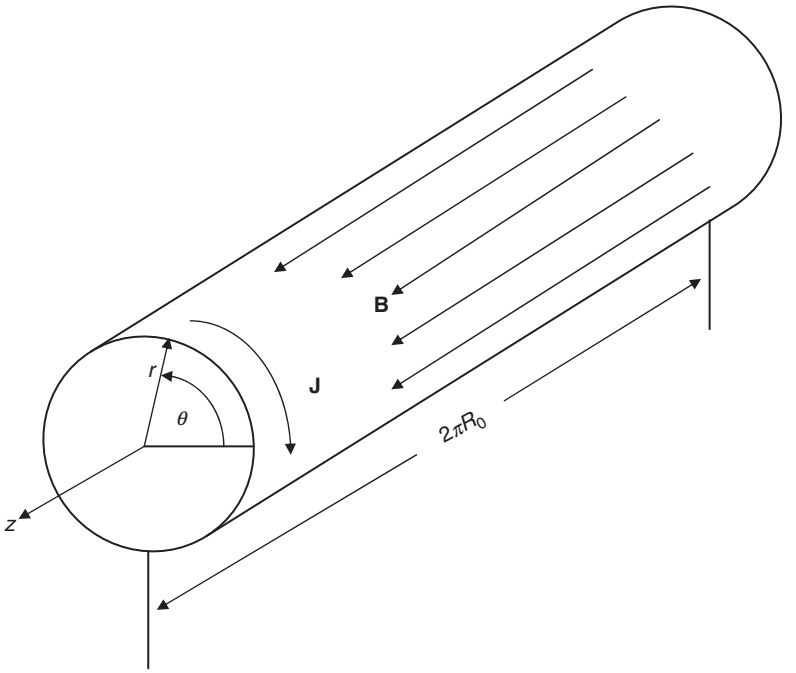

Figure 5.1 Linear θ-pinch geometry.

in length of the infinitely long cylindrically symmetric linear plasma column. In a θ-pinch the only non-zero component of $\mathbf{B}$ is in the z direction: $\mathbf{B} = B_z(r)\mathbf{e}_z$. It is applied externally and induces a large diamagnetic current in the θ direction: $\mathbf{J} = J_\theta(r)\mathbf{e}_\theta$. The resulting $\mathbf{J} \times \mathbf{B}$ force confines the pressure $p(r)$. See Fig. 5.1 for the geometry. The θ directed current is the origin of the name θ-pinch.

The basic equilibrium relation for a θ-pinch is easily obtainable from the radial component of the momentum equation. However, a slightly more formal derivation is presented which demonstrates the general procedure used for all one- and two-dimensional MHD configurations discussed in the textbook. Specifically, there is a natural sequence in which to solve the MHD equations which provides a simple and direct path to the final equations of interest. This sequence is given by (1) the $\nabla \cdot \mathbf{B} = 0$ equation, (2) Ampere's law, and (3) the momentum equation:

- $\nabla \cdot \mathbf{B} = 0$: The equation $\nabla \cdot \mathbf{B} = 0$ is trivially satisfied for the θ-pinch because of symmetry; all quantities are only a function of the radial coordinate r.

$$\nabla \cdot \mathbf{B} = 0 \quad \rightarrow \quad \frac{\partial B_z}{\partial z} = 0 \tag{5.1}$$

- **Ampere's law:** Ampere's law shows that only $J_\theta(r)$ is non-zero.

$$\mathbf{J} = \frac{1}{\mu_0}\nabla \times \mathbf{B} \quad \rightarrow \quad J_\theta = -\frac{1}{\mu_0}\frac{dB_z}{dr} \tag{5.2}$$

- **Momentum equation:** The only non-trivial component of the momentum equation is in the radial direction and is given by

$$\mathbf{J} \times \mathbf{B} = \nabla p \quad \rightarrow \quad J_\theta B_z = \frac{dp}{dr} \tag{5.3}$$

Here, the pressure $p = p(r)$. Eliminating J_θ by means of Eq. (5.2) leads to

$$\frac{d}{dr}\left(p + \frac{B_z^2}{2\mu_0}\right) = 0 \tag{5.4}$$

This equation can be easily integrated, yielding

$$p + \frac{B_z^2}{2\mu_0} = \frac{B_0^2}{2\mu_0} \tag{5.5}$$

where B_0 is the applied magnetic field.

Equation (5.4) is the basic radial pressure balance relation for a θ-pinch. Its integrated form given by Eq. (5.5) indicates that at any local value of r the sum of the local particle pressure plus local magnetic pressure is a constant, equal to the externally applied magnetic pressure. The conclusion is that in a θ-pinch radial pressure balance is achieved by the pressure exerted by the externally applied magnetic field.

Illustrated in Fig. 5.2 is a set of typical profiles given, for example, by

$$\begin{aligned}
\frac{2\mu_0 p(r)}{B_0^2} &= 1 - \left[1 - \hat{\beta}\left(1-\rho^2\right)^2\right]^2 \\
\frac{B_z(r)}{B_0} &= 1 - \hat{\beta}\left(1-\rho^2\right)^2 \\
\frac{a\mu_0 J_\theta(r)}{B_0} &= -4\hat{\beta}\rho\left(1-\rho^2\right) \\
\hat{\beta} &= \frac{\beta_0}{1 + (1-\beta_0)^{1/2}}
\end{aligned} \tag{5.6}$$

where $\rho = r/a$ and $\beta_0 = 2\mu_0 p_0/B_0^2$ is defined as the beta on axis. For physical solutions $\beta_0 < 1$. The pressure peaks at $r = 0$ and vanishes at the plasma edge $r = a$ (i.e., $\rho = 1$). The profiles are chosen so that the current density and pressure

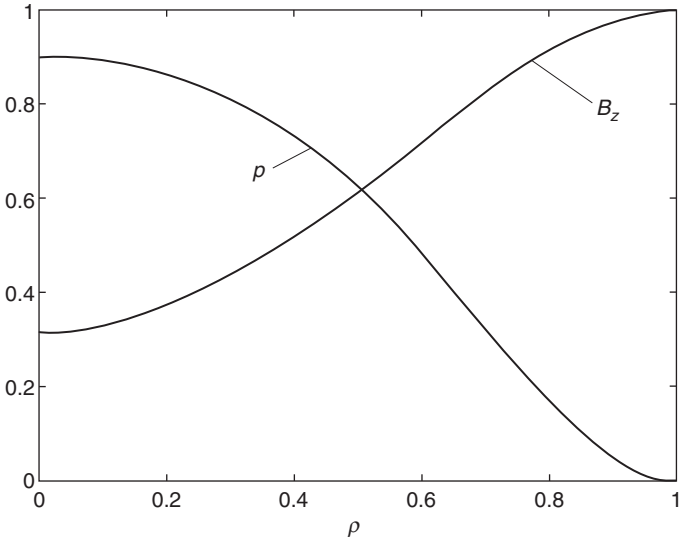

Figure 5.2 Equilibrium profiles for a θ-pinch.

gradient also vanish at $r = a$. The plasma is thus isolated from the containing wall indicating good radial confinement and closed, nested pressure contours.

Note that Eq. (5.4) implies that the θ-pinch has one free surface function, for example $B_z(r)$, from which it is then possible to calculate $p(r)$. The second free function (e.g., $B_\theta(r)$) has been set to zero because of the special symmetry associated with the θ-pinch.

The basic plasma parameters and figures of merit can now be easily evaluated. Consider first the value of beta. Since $B_\theta = 0$, then $\beta = \beta_t$ with the toroidal β given by Eq. (4.19)

$$\begin{aligned}\beta_t &= \frac{2\mu_0\langle p\rangle}{B_0^2}\\ &= \frac{4\mu_0}{a^2B_0^2}\int_0^a pr\,dr\\ &= 2\int_0^1\left(1-\frac{B_z^2}{B_0^2}\right)\rho\,d\rho\\ &= \hat{\beta}\left(\frac{2}{3}-\frac{\hat{\beta}}{5}\right)\end{aligned} \tag{5.7}$$

where the last expression corresponds to the profiles given by Eq. (5.6). Note that as $\beta_0 \to 0$ then $\hat{\beta} \approx \beta_0/2$ and $\beta_t \approx \beta_0/3$. Similarly, as $\beta_0 \to 1$ then $\hat{\beta} \to 1$ and $\beta_t \approx 7/15$.

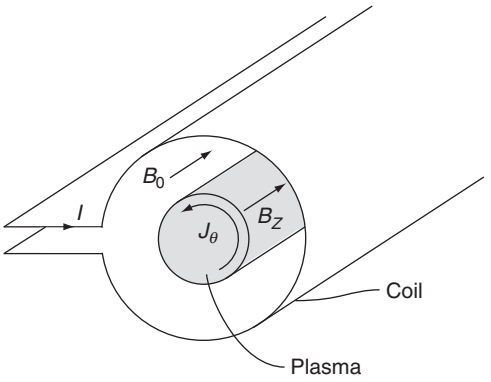

Figure 5.3 Schematic diagram of a θ-pinch experiment.

Equation (5.7) implies that, in general, physical profiles can exist for

$$0 < \beta_t < 1 \tag{5.8}$$

This wide range of variation including access to high values of β_t indicates that the θ-pinch is an excellent option for producing radial pressure balance in a fusion plasma.

Furthermore, since there is no z current in a θ-pinch (i.e., $I = 0$) then $\beta_p = \infty$ and as such is not a relevant quantity. Similarly, $q_* = \infty$ indicating favorable stability against current-driven kink modes, which is a trivial result since there is no toroidal current. The local safety factor $q(r) = \infty$, again a consequence of no z current.

The θ-pinch is more than a theoretical concept and in the early years of the fusion program a number of such devices were built. The typical experimental situation is illustrated in Fig. 5.3. The plasma fills an insulating discharge tube (usually made of quartz or Pyrex), which is surrounded by a single turn coil connected to a large capacitor bank. The gas is initially pre-ionized after which the switch on the capacitor bank is closed. As the capacitor discharges, current flows in the coil, producing a B_z field in the discharge chamber. The parameters of the high-voltage capacitor bank are chosen so that the rise time of the field is quite short, on the order of 2 μsec, while the overall pulse length is typically 10 μsec. The rapidly rising magnetic field acts like a piston, imparting a large impulse of momentum and energy to the particles as they are reflected off the piston face. This energy is ultimately converted to heat after repeated reflections off the converging piston.

The performance of θ-pinches in terms of fusion parameters represents one of the early successes of the fusion program. Using the implosion heating method, ion temperatures of 1–4 keV were routinely obtained at very high density, $n \sim 1\text{–}2 \times 10^{22}\,\mathrm{m}^{-3}$. The peak value of beta on axis was typically $\beta_0 \sim 0.7\text{–}0.9$, quite a high

value, but corresponding to a volume averaged beta of only $\beta_t \sim 0.05$. The low average beta was a consequence of the large compression ratio of the plasma due to the implosion heating. This type of heating left a large volume of very low pressure plasma between the plasma core and the wall. As further evidence of good performance, radial profile measurements made by end-on holographic interferometry demonstrated excellent radial confinement, nested circular flux surfaces, and no indications of macroscopic instability. Because of the high temperatures and densities, the θ-pinch was the first laboratory device to successfully produce a substantial number of thermonuclear neutrons.

As might be expected, the biggest problem with the θ-pinch was end loss. Typically, little if anything was done to provide axial confinement of particles or energy; the plasma simply flowed out the end of the device along field lines in a characteristic time $\tau = L/V_{Ti}$, where L is the length of the magnet. For a 5-m device, $\tau \sim 10\,\mu$sec, a very short time indeed. Because of the end-loss problem the θ-pinch has been replaced by more advanced toroidal concepts capable of much longer confinement times.

Before closing the discussion of θ-pinches, several comments should be made regarding toroidal equilibrium and stability. The cylindrical θ-pinch represents a highly degenerate configuration for the following reasons. A complete and detailed stability analysis indicates that the straight θ-pinch is marginally stable against the most dangerous MHD modes. It is never unstable. Also, as has been previously shown, the θ-pinch cannot be bent into a torus. Therefore, small additional fields, of order a/R_0, must be added to provide toroidal force balance. Since the basic straight configuration is marginally stable, the overall stability depends sensitively on these small, as yet unidentified, additional fields. Thus, the important problems have yet to be faced.

5.3 The *Z*-pinch

The Z-pinch is a one-dimensional model of the toroidal configuration with purely poloidal field and is in many ways orthogonal to the θ-pinch. In a Z-pinch, the only non-zero field component is $B_\theta(r)$ and consists entirely of the self-field induced by the longitudinal current $J_z(r)$ flowing in the plasma; hence the name Z-pinch.[1] Again the $\mathbf{J} \times \mathbf{B}$ force confines the pressure $p(r)$ (see Fig. 5.4). Unlike the θ-pinch, when the total plasma current vanishes there is no remaining background $\mathbf{B}$ field. The basic equation describing radial pressure balance in a Z-pinch is determined as follows:

[1] Note this does not violate the virial theorem since the current is not confined in that it extends from $-\infty < z < \infty$.

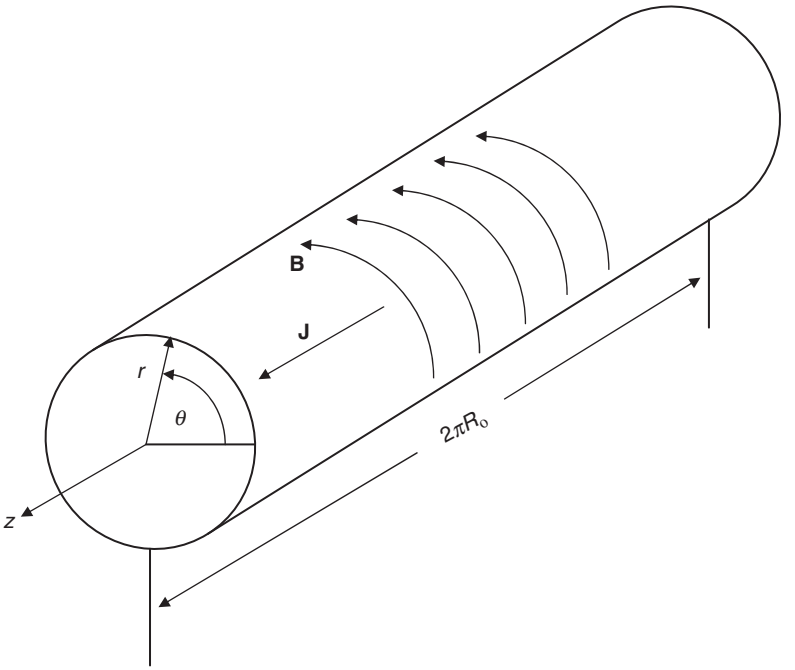

Figure 5.4 Linear Z-pinch geometry.

- $\nabla \cdot \mathbf{B} = 0$: As for the θ-pinch the $\nabla \cdot \mathbf{B} = 0$ equation is trivially satisfied because of symmetry; all quantities are only functions of r.

$$\nabla \cdot \mathbf{B} = 0 \quad \rightarrow \quad \frac{1}{r}\frac{\partial B_\theta}{\partial \theta} = 0 \tag{5.9}$$

- **Ampere's law:** Application of Ampere's law shows that only $J_z(r)$ is non-zero.

$$\mathbf{J} = \frac{1}{\mu_0}\nabla \times \mathbf{B} \quad \rightarrow \quad J_z = \frac{1}{\mu_0 r}\frac{d}{dr}(rB_\theta) \tag{5.10}$$

- **Momentum equation:** Only the radial component of the momentum equation yields non-trivial information

$$\mathbf{J} \times \mathbf{B} = \nabla p \quad \rightarrow \quad J_z B_\theta = -\frac{dp}{dr} \tag{5.11}$$

The radial pressure balance relation is obtained by substituting J_z from Eq. (5.10). The result is

$$\frac{dp}{dr} + \frac{B_\theta}{\mu_0 r}\frac{d}{dr}(rB_\theta) = 0 \tag{5.12}$$

which can be rewritten as

$$\frac{d}{dr}\left(p+\frac{B_\theta^2}{2\mu_0}\right)+\frac{B_\theta^2}{\mu_0 r}=0 \tag{5.13}$$

Equation (5.13) is the basic radial pressure balance relation for a Z-pinch. The two terms in the derivative represent the particle pressure and the magnetic pressure. The last term represents the tension force generated by the curvature of the magnetic field lines. The connection between the tension force and the curvature is a general result obtained by substituting $\mathbf{J}$ from Ampere's law directly into the momentum equation for arbitrary 3-D magnetic configurations. Noting that $(\nabla\times\mathbf{B})\times\mathbf{B}=-\nabla(B^2/2)+\mathbf{B}\cdot\nabla\mathbf{B}$ and defining $\boldsymbol{\kappa}=\mathbf{b}\cdot\nabla\mathbf{b}$ with $\mathbf{B}=B\mathbf{b}$ one finds

$$\nabla_\perp\left(p+\frac{B^2}{2\mu_0}\right)-\frac{B^2}{\mu_0}\boldsymbol{\kappa}=0 \tag{5.14}$$

The quantity $\boldsymbol{\kappa}$ is known as the curvature vector and is related to the radius of curvature vector $\mathbf{R}_c$ by $\boldsymbol{\kappa}=-\mathbf{R}_c/R_c^2$. For readers unfamiliar with this relation, a derivation is presented in Appendix D. Now, since $\boldsymbol{\kappa}=\mathbf{e}_\theta\cdot\nabla\mathbf{e}_\theta=-\mathbf{e}_r/r$ in a Z-pinch, the connection between the tension force and curvature is apparent.

The tension force is very important. In contrast to a θ-pinch, for a Z-pinch it is the tension force and not the magnetic pressure gradient that provides radial pressure balance. This can be seen explicitly from an example. It can be easily verified that the profiles below, for which p, ∇p, and J_z all vanish at the plasma edge $r=a$, satisfy the Z-pinch pressure balance relation:

$$\begin{aligned}\frac{2\mu_0 p(r)}{B_{\theta a}^2}&=\frac{2}{3}\left(5-2\rho^2\right)\left(1-\rho^2\right)^2\\ \frac{B_\theta(r)}{B_{\theta a}}&=2\rho\left(1-\rho^2/2\right)\\ \frac{a\mu_0 J_z(r)}{B_{\theta a}}&=4\left(1-\rho^2\right)\end{aligned} \tag{5.15}$$

Here, $\rho=r/a$, $B_{\theta a}\equiv B_\theta(a)=\mu_0 I/2\pi a$, and I is the total current flowing in the plasma. These profiles are illustrated in Fig. 5.5. Also illustrated are curves of $-p'$, $-(B_\theta^2/2\mu_0)'$, and $-B_\theta^2/\mu_0 r$ vs. r, representing the outward force density profiles of the three contributions to radial pressure balance. Note that in the outer region of the plasma, $r/a>(2/3)^{1/2}$, the plasma and magnetic pressure gradients are both pointing outward; the plasma is not confined by magnetic pressure. Instead it is the tension force that acts inwards, thereby providing radial pressure balance. If one thinks of the magnetic lines as rubber bands wrapped around the plasma column,

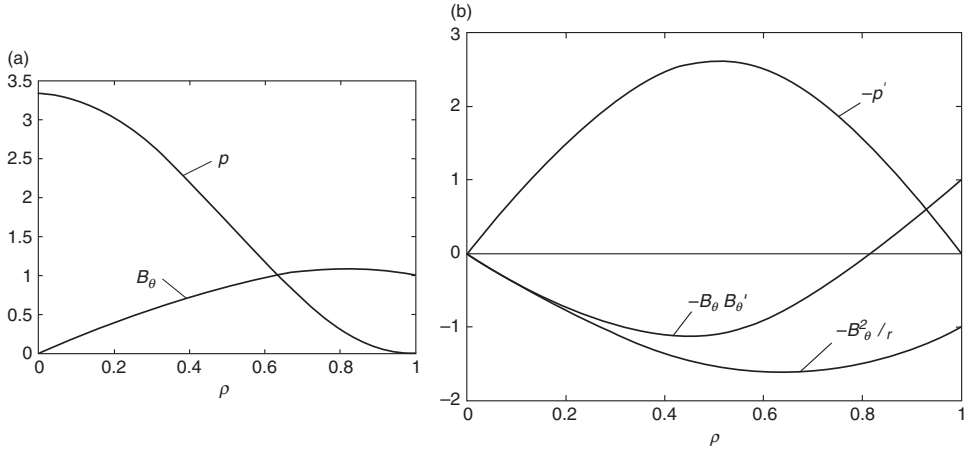

Figure 5.5 Equilibrium profiles for a Z-pinch: (a) $2\mu_0 p/B_{\theta a}^2$ and $B_\theta/B_{\theta a}$, (b) outward forces $-p'$, $-(B_\theta^2/2\mu_0)'$, and $-B_\theta^2/\mu_0 r$

then the tension force is obvious. In analogy with the θ-pinch, the Z-pinch equilibrium has one free function, for instance $B_\theta(r)$, which then determines $p(r)$. The other free function, $B_z(r)$, has been set to zero because of the special Z-pinch symmetry.

From the basic Z-pinch relationships given by Eqs. (5.10)–(5.13) it is straightforward to calculate the plasma parameters and figures of merit. First, since $B_z = 0$ the plasma beta reduces to $\beta = \beta_p$. Using the form of β_p given by Eq. (4.19), it follows that β_p reduces to

$$\begin{aligned}\beta_p &= \frac{2\mu_0\langle p\rangle}{B_{\theta a}^2} \\ &= \frac{4\mu_0}{a^2 B_{\theta a}^2}\int_0^a pr\,dr \\ &= 1\end{aligned} \tag{5.16}$$

The result $\beta_p = 1$ is known as the Bennett pinch relation (1934) and is actually valid for any confined Z-pinch profile. While high β_p is desirable for confinement efficiency, the lack of flexibility in achieving small to moderate β_p is a disadvantage; that is, some classes of potentially dangerous MHD modes might be stabilized if β_p could be lowered. The fact that this cannot occur in a pure Z-pinch is one reason why its stability properties are so poor.

Since $B_z = 0$ for a Z-pinch, the quantities β_t, q_* and $q(r)$ approach limiting values. The toroidal beta has the value $\beta_t = \infty$ and as such is not a relevant quantity. The kink safety factor $q_* = 0$, indicating poor stability against current-driven kinks. Also, since the magnetic field line trajectories never progress along z it follows that $q(r) = 0$.

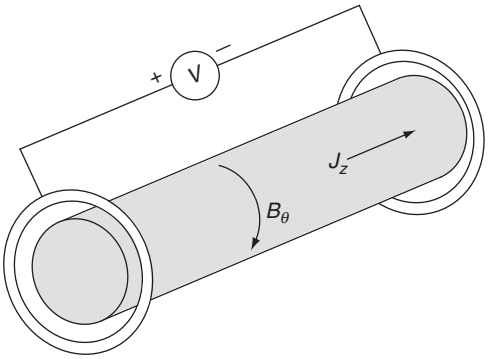

Figure 5.6 Schematic diagram of a linear *Z*-pinch experiment.

A number of linear *Z*-pinch experiments were constructed during the early years of the fusion program. A typical device is illustrated schematically in Fig. 5.6. Here, a capacitor bank is discharged across two electrodes located at each end of a cylindrical quartz or Pyrex tube. The high voltage ionizes the gas and produces a z current flowing along the plasma. These early experiments exhibited disastrous instabilities, often leading to a complete quenching of the plasma after 1–2 μsec. This behavior is discussed in detail in Chapter 11 and is consistent with the unfavorable figures of merit derived above.

Finally, with regard to toroidal equilibrium, recall that the *Z*-pinch can easily be bent into a torus, although its stability properties remain poor. An interesting innovation to the simple *Z*-pinch is the addition of a current-carrying conductor along the axis which greatly improves stability. This configuration is known as the hard-core *Z*-pinch.

5.4 The general screw pinch

5.4.1 General properties

It should come as no great surprise that the search for MHD stable toroidal equilibria has led to configurations that combine toroidal and poloidal fields. The hope, of course, is to combine the favorable features of each field while suppressing the unfavorable ones. The one-dimensional analogs of such systems have both $B_\theta(r)$ and $B_z(r)$ being non-zero (see Fig. 5.7). The basic pressure balance relation for a general screw pinch follows in a straightforward manner.

- $\nabla \cdot \mathbf{B} = 0$: Even with two field components present, cylindrical symmetry guarantees that $\nabla \cdot \mathbf{B} = 0$ is trivially satisfied.

$$\nabla \cdot \mathbf{B} = 0 \quad \rightarrow \quad \frac{1}{r}\frac{\partial B_\theta}{\partial \theta} + \frac{\partial B_z}{\partial z} = 0 \tag{5.17}$$

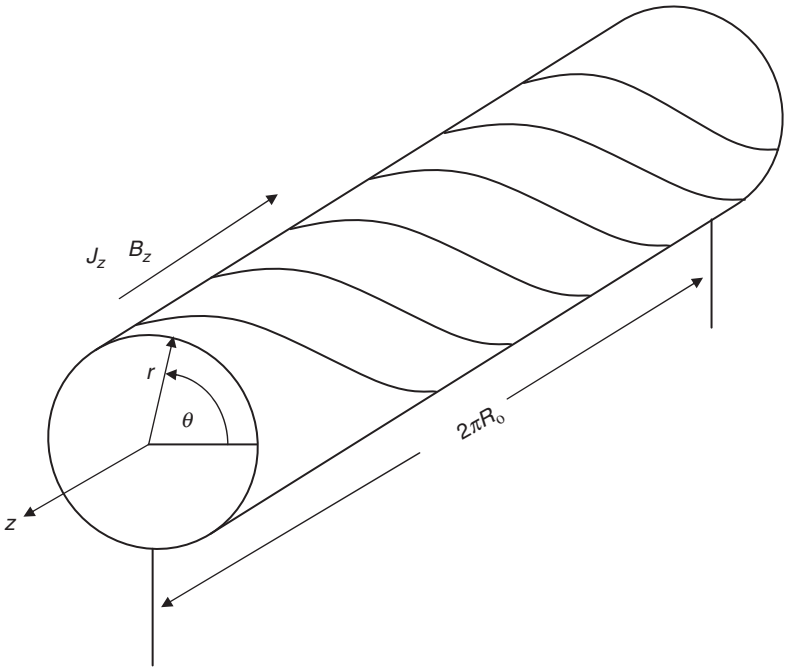

Figure 5.7 General screw pinch geometry.

- **Ampere's law:** Application of Ampere's law shows that two components of current, $J_\theta(r)$ and $J_z(r)$, are non-zero.

$$\mathbf{J} = \frac{1}{\mu_0}\nabla \times \mathbf{B} \quad \rightarrow \quad \mathbf{J} = \frac{1}{\mu_0 r}\frac{d}{dr}(rB_\theta)\mathbf{e}_z - \frac{1}{\mu_0}\frac{dB_z}{dr}\mathbf{e}_\theta \tag{5.18}$$

- **Momentum equation:** As before, only the radial component of the momentum equation is non-trivial.

$$\mathbf{J} \times \mathbf{B} = \nabla p \quad \rightarrow \quad J_\theta B_z - J_z B_\theta = \frac{dp}{dr} \tag{5.19}$$

Substituting Eq. (5.18) yields

$$\frac{d}{dr}\left(p + \frac{B_\theta^2 + B_z^2}{2\mu_0}\right) + \frac{B_\theta^2}{\mu_0 r} = 0 \tag{5.20}$$

Equation (5.20) is the basic radial pressure balance relation for a general screw pinch. Note that even though the momentum equation is non-linear, the θ-pinch and Z-pinch forces superpose linearly, a consequence of the cylindrical symmetry. Although Eq. (5.20) is a relatively simple relation, it nevertheless exhibits many of the features and flexibility expected in more realistic, multidimensional,

toroidal models. This is demonstrated by examining Eq. (5.20) and evaluating the corresponding plasma parameters and figures of merit.

- **Free functions:** There are two free functions available to specify the equilibrium; for example, $B_\theta(r)$ and $B_z(r)$. The θ-pinch and Z-pinch are special choices where B_θ or B_z is set to zero, respectively. In the general case, once both profiles are specified, the pressure is calculated from Eq. (5.20).
- **Flux surfaces:** The contours of constant pressure are given by $r =$ constant. Thus, the flux surfaces consist of closed concentric circles.
- **Beta:** The value of β can vary over a wide range if B_z is not zero. This can be seen from the general one-dimensional macroscopic force balance in the plasma. The relation is obtained by multiplying Eq. (5.20) by r^2 and integrating over the plasma from $0 < r < a$. A short calculation yields a volume averaged radial pressure balance relation which can be written in two equivalent forms

$$\begin{aligned} 2\pi\int_0^a prdr &= \frac{\mu_0 I^2}{8\pi} + 2\pi\int_0^a \frac{B_0^2 - B_z^2}{2\mu_0}\, rdr \\ \langle p\rangle &= \frac{B_{\theta a}^2}{2\mu_0} + \frac{1}{2\mu_0}\left(B_0^2 - \langle B_z^2\rangle\right) \end{aligned} \tag{5.21}$$

The second form is obtained by multiplying the first by $1/\pi a^2$ and using the definition of volume average.

The left-hand term in Eq. (5.21) represents the outward force due to the plasma pressure. The first right-hand term represents the inward force due to the magnetic tension in the poloidal field. The last term represents the net force due to the magnetic pressure of the toroidal field. It can be inward or outward depending on whether the plasma is diamagnetic or paramagnetic with respect to the toroidal field. If one now recalls the simplified definitions of β_t, β_p, and β from Eqs. (4.18)–(4.20) which are given by

$$\begin{aligned} \beta_t &= \frac{2\mu_0}{B_0^2}\langle p\rangle \\ \beta_p &= \frac{2\mu_0}{B_{\theta a}^2}\langle p\rangle \\ \beta &= \frac{\beta_t\beta_p}{\beta_t + \beta_p} \end{aligned} \tag{5.22}$$

it then follows that

$$\beta = \frac{2\mu_0\langle p\rangle}{B_0^2 + B_{\theta a}^2} \tag{5.23}$$

Clearly $\beta < 1$ and can vary over a large range depending on the size of B_0.

- **Kink safety factor:** The kink safety factor is readily evaluated from Eq. (4.21) and is given by

$$q_* = \frac{2\pi a^2 B_0}{\mu_0 R_0 I} = \frac{aB_0}{R_0 B_{\theta a}} \tag{5.24}$$

Its value can vary over a wide range depending on the ratio of toroidal field to toroidal current and the geometry a/R_0.

- **Rotational transform and safety factor:** The magnetic field lines wrap around the column along helical paths similar to the stripes on a barber pole (see Fig. 5.7). This gives rise to a non-zero rotational transform. The value of ι is calculated by noting that the angle $\Delta\theta$ defined in Eq. (4.26) is independent of the starting angle θ_0 because of the cylindrical symmetry. Consequently, to calculate ι it is only necessary to integrate the field line trajectory a distance $\Delta z = 2\pi R_0$ corresponding to one transit around the equivalent torus.

$$\iota = \Delta\theta = \int_0^{\Delta\theta} d\theta = \int_0^{2\pi R_0} \frac{d\theta}{dz} \quad dz \tag{5.25}$$

From the equations for the field line trajectories

$$\begin{aligned} \frac{dr}{dz} &= \frac{B_r(r)}{B_z(r)} = 0 \\ \frac{d\theta}{dz} &= \frac{B_\theta(r)}{rB_z(r)} \end{aligned} \tag{5.26}$$

one sees from the first of these that $r =$ constant, indicating circular flux surfaces. After substituting the second relation into Eq. (5.25) it follows that the expression for ι given by Eq. (5.25) can be trivially integrated yielding

$$\iota(r) = \frac{2\pi R_0 B_\theta(r)}{rB_z(r)} \tag{5.27}$$

The safety factor $q(r) = 2\pi/\iota(r)$ can thus be written as

$$q(r) = \frac{rB_z(r)}{R_0 B_\theta(r)} \tag{5.28}$$

Again, with two free functions available, there is a wide range of flexibility in the $q(r)$ profile. In general, the magnetic shear will be non-zero. Also, note that for a screw pinch $q(a) = q_*$.

This completes the discussion of the plasma parameters and figures of merit for the screw pinch. By now it should be clear that a wide variety of fusion

configurations are described by the general pressure balance relation given by Eq. (5.20). For purposes of illustration it is useful to describe two limiting conceptual examples of screw pinch equilibria which bracket the configurations of interest. These are the parallel pinch and the perpendicular pinch, and are discussed below. More interestingly, two actual present day fusion configurations, the reversed field pinch and the low β ohmic tokamak, are accurately described by the 1-D screw pinch equilibrium relation and these are discussed in Sections 5.5.2 and 5.5.3.

5.4.2 The parallel pinch

The parallel pinch is a configuration in which all the current flows parallel to the magnetic field. In other words, $\mu_0\mathbf{J} = k(r)\mathbf{B}$, where $k(r)$ is an arbitrary scalar function. Since $\mathbf{J}$ is parallel to $\mathbf{B}$ there is no magnetic force $\mathbf{J} \times \mathbf{B}$ acting on the plasma and for obvious reasons such configurations are often called "force free." Furthermore, since $\mathbf{J} \times \mathbf{B} = 0$, the pressure $p(r) = 0$ everywhere. Force-free configurations are good approximations to very low β systems. For the parallel pinch it is instructive to calculate the magnetic field profiles as well as $q(r)$. The goal is to learn whether or not confined current density profiles exist with a high value of kink safety factor $q_* \sim 1$. The analysis proceeds as follows and is more complicated than one might expect.

The basic equilibrium equation for the parallel pinch is obtained by substituting $d(rB_\theta)/dr = krB_z$ into Eq. (5.20) yielding

$$\frac{r}{k}\frac{dB_z}{dr} = -rB_\theta \tag{5.29}$$

This equation is now differentiated with respect to r after which $d(rB_\theta)/dr$ is again eliminated. The result is a single differential equation for B_z given by

$$\frac{1}{rk}\frac{d}{dr}\left[\frac{r}{k}\frac{dB_z}{dr}\right] + B_z = 0 \tag{5.30}$$

One simple solution to this equation corresponds to the choice $k(r) = k_0 =$ constant. In this case the solutions are given by

$$\begin{aligned} B_z &= \frac{\mu_0 J_z}{k_0} = B_0 \mathrm{J}_0(k_0 r) \\ B_\theta &= \frac{\mu_0 J_\theta}{k_0} = B_0 \mathrm{J}_1(k_0 r) \end{aligned} \tag{5.31}$$

where $B_0 =$ constant and J_0, J_1 (in Roman, not italic fonts) are Bessel functions. This solution is not entirely satisfactory since the current density is finite at the edge of the plasma $r = a$. It is not confined.

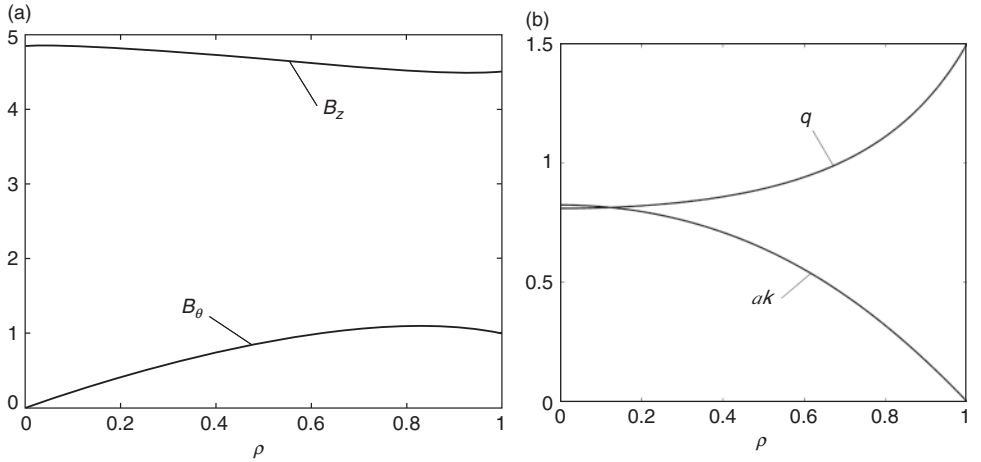

Figure 5.8 Equilibrium profiles for the parallel pinch for the case $\alpha = 2/9$ and $q_* = 3/2$. Illustrated are (a) $B_\theta/B_{\theta a}$ and $B_z/B_{\theta a}$, (b) ak and q.

However, Eq. (5.30) is difficult to solve analytically, even for simple choices of $k(r)$ describing confined equilibria. Such equilibria require $\mu_0 J_z(0) = k(0)B_z(0) =$ constant and $\mu_0 J_z(0) = k(a)B_z(a) = 0$. The corresponding $k(r)$ must satisfy $k(0) =$ constant and $k(a) = 0$. An alternate way to approach the problem is to specify a plausible profile for $\mu_0 J_z(r) = k(r)B_z(r)$ and then use Eq. (5.30) to calculate $k(r)$. A plausible choice for $J_z(r)$ is as follows:

$$J_z(r) = \frac{4B_{\theta a}}{\mu_0 a}\left(1-\rho^2\right) \tag{5.32}$$

where again $\rho = r/a$. After a slightly tedious calculation the unintuitive $k(r)$ can be evaluated and then back substituted to obtain the desired profiles:

$$\begin{aligned}
ak(\rho) &= \frac{4\alpha(1-\rho^2)}{\left[1+(2\alpha^2/3)(1-\rho^2)^2(5-2\rho^2)\right]^{1/2}} \\
\frac{B_\theta(\rho)}{B_{\theta a}} &= \frac{\mu_0 J_\theta(\rho)}{B_{\theta a}k(\rho)} = \rho(2-\rho^2) \\
\frac{B_z(\rho)}{B_{\theta a}} &= \frac{\mu_0 J_z(\rho)}{B_{\theta a}k(\rho)} = \frac{1}{\alpha}\left[1+(2\alpha^2/3)(1-\rho^2)^2(5-2\rho^2)\right]^{1/2} \\
q(\rho) &= \frac{q_*}{2-\rho^2}\left[1+(2\alpha^2/3)(1-\rho^2)^2(5-2\rho^2)\right]^{1/2}
\end{aligned} \tag{5.33}$$

Here, $B_{\theta a} = B_\theta(a)$, $B_z(a) = B_0$, and $\alpha = B_{\theta a}/B_0 = \varepsilon/q_*$.

The profiles are illustrated in Fig. 5.8 for the case $q_* = 3/2$ and $\varepsilon = 1/3$ corresponding to $\alpha = 2/9$. Observe that $B_z(0)/B_z(a) = 1 + (10/3)\,\alpha^2 \approx 1.16 > 1$,

showing that the toroidal field is paramagnetic. In fact it can be easily shown that any force-free equilibrium must be paramagnetic with respect to the toroidal magnetic field. This follows by setting $p = 0$ in the general force balance relation given by Eq. (5.21):

$$\text{Paramagnetism} \equiv 2\pi \int_0^a \frac{B_z^2 - B_0^2}{2\mu_0} r dr = \frac{\mu_0 I^2}{8\pi} > 0 \tag{5.34}$$

The safety factor profile can either increase or decrease with radius. For the profiles in the example the transition point is $\alpha^2 = 9/10$ with smaller values corresponding to an increasing q profile. Specifically, one finds $q(0)/q(a) = [1 + (5/6)(\alpha^2 - 9/10)]^{1/2}$.

The conclusion is that force-free solutions can be found that describe equilibria with confined current densities and high values of the kink safety factor.

5.4.3 The perpendicular pinch

The perpendicular pinch is a configuration in which all the current flows perpendicular to the magnetic field. There is no parallel current: $\mathbf{J} \cdot \mathbf{B} = 0$. One might anticipate that this configuration confines the maximum amount of pressure since no current is "wasted" flowing parallel to the field, which would produce no force on the plasma. The goal of the example below is to calculate typical profiles for the perpendicular pinch and to see how large β can become assuming that the kink safety factor is large, of order unity.

The analysis begins by noting that $\mathbf{J} \cdot \mathbf{B} = 0$ implies that

$$\frac{1}{B_z}\frac{dB_z}{dr} = \frac{1}{rB_\theta}\frac{d}{dr}(rB_\theta) \tag{5.35}$$

This equation can be easily integrated yielding

$$B_z(\rho) = B_0 \frac{\rho B_\theta(\rho)}{B_{\theta a}} \tag{5.36}$$

Assume now that a confined $J_z(\rho)$ profile is specified. Plausible choices for $J_z(\rho)$ and the corresponding $B_\theta(\rho)$ are as follows:

$$\begin{aligned} \frac{a\mu_0 J_z(\rho)}{B_0} &= \frac{4\varepsilon}{q_*}\left(1 - \rho^2\right) \\ \frac{B_\theta(\rho)}{B_0} &= \frac{\varepsilon}{q_*}\rho\left(2 - \rho^2\right) \end{aligned} \tag{5.37}$$

where $B_{\theta a}/B_0 = \varepsilon/q_*$. The $B_z(\rho)$ and $J_\theta(\rho)$ profiles are now easily calculated from Eq. (5.36)

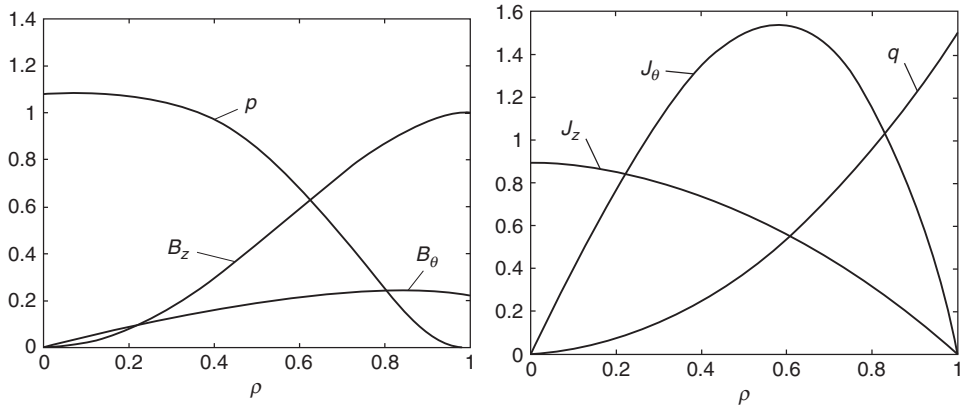

Figure 5.9 Equilibrium profiles for the perpendicular pinch for the case $q_* = 3/2$ and $\varepsilon = 1/3$: (a) B_z/B_0, B_θ/B_0, $2\mu_0 p/B_0^2$ and (b) $a\mu_0 J_z/B_0$, $a\mu_0 J_\theta/B_0$, q.

$$\frac{B_z(\rho)}{B_0} = \rho^2\left(2-\rho^2\right)$$
$$\frac{a\mu_0 J_\theta(\rho)}{B_0} = 4\rho\left(1-\rho^2\right) \tag{5.38}$$

Knowing B_z and B_θ, one can evaluate the safety factor

$$q(\rho) = q_*\rho^2 \tag{5.39}$$

The last step is to determine $p(\rho)$ from Eq. (5.20), the radial pressure balance relation. A short calculation leads to

$$\frac{2\mu_0 p(\rho)}{B_0^2} = \left(1-\rho^2\right)^2\left[1+2\rho^2-\rho^4+\frac{\varepsilon^2}{3q_*^2}\left(5-2\rho^2\right)\right] \tag{5.40}$$

The profiles are plotted in Fig. 5.9 for the case $q_* = 3/2$ and $\varepsilon = 1/3$. Note that $B_z(0) = 0$, indicating that the toroidal field is highly diamagnetic. Similarly $q(0) = 0$. Thus, while high values of q_* are allowed, one should be concerned that the safety factor on axis is always zero, a warning sign of potential internal instabilities.

The original question can now be addressed – how large can β become assuming $q_* \sim 1$? From the definition of β given by Eq. (5.23), one can show after a short calculation that

$$\beta = \frac{2\mu_0\langle p\rangle}{B_0^2 + B_{\theta a}^2} = \frac{1}{30}\left(\frac{14+15\varepsilon^2/q_*^2}{1+\varepsilon^2/q_*^2}\right) \tag{5.41}$$

The value of β is almost independent of q_* and is approximately given by $\beta \approx 1/2$. This is indeed a high value, although it will be shown in Chapter 6 that the

inclusion of toroidal force balance effects reduces the achievable β by a substantial amount when $q_* \sim 1$.

5.5 Inherently 1-D fusion configurations

There are two present day fusion configurations whose MHD equilibrium and stability are accurately described by a 1-D model: the reversed field pinch, and the low β ohmic tokamak with circular cross section. For these configurations toroidal effects enter only perturbatively when calculating toroidal force balance and do not have a qualitative impact on MHD stability. Radial pressure balance in other configurations such as the high β auxiliary heated tokamak and the stellarator can also be described by the 1-D screw pinch model but in these cases toroidicity qualitatively alters both toroidal force balance and MHD stability. For this reason discussions of the equilibrium properties of these configurations are postponed until multidimensional systems are analyzed in Chapters 6 and 7.

Consider now the MHD equilibrium properties of the two inherently 1-D configurations.

5.5.1 The reversed field pinch

Overview

The reversed field pinch (RFP) is an axisymmetric toroidal configuration with comparably sized toroidal and poloidal magnetic fields. The plasma pressure is high, similar in magnitude to the magnetic pressures. The aspect ratio $R_0/a \sim 5$ is relatively large compared to many other fusion configurations. An important feature of the RFP is that the toroidal field coils are very modest in size, a distinct technological advantage with respect to complexity and cost as one looks ahead to reactors.

Carefully tailored, and sometimes naturally occurring, pressure and current profiles are stable to macroscopic MHD modes localized internally within the plasma. For these "internal" modes the plasma surface does not move. However, "external" modes where the plasma surface is allowed to move are always MHD unstable and require a close fitting conducting shell around the plasma and/or feedback for stability. Research has also shown that under certain circumstances the plasma deforms from its "unstable" cylindrical shape into a "stable" helically shaped plasma. The present discussion is focused on cylindrical RFP equilibria.

There are several main RFP experiments currently in operation around the world: (1) the Madison Symmetric Torus (MST) at the University of Wisconsin

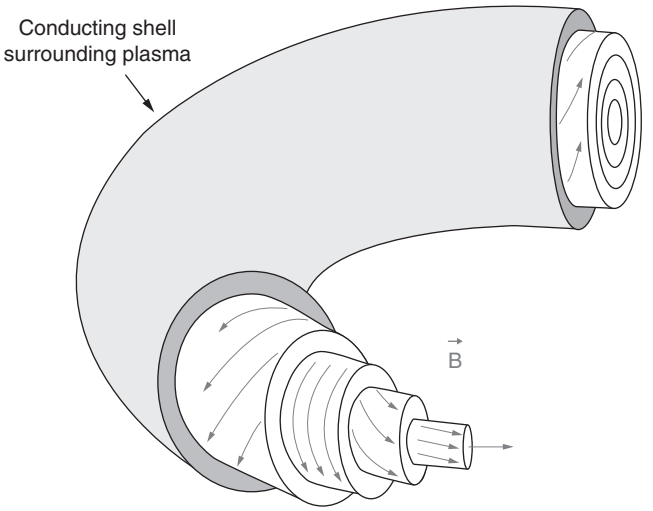

Figure 5.10 Schematic diagram of an RFP (courtesy of J. S. Sarff).

(USA); (2) the Reversed Field Experiment (RFX) operated by an Italian consortium consisting of the University of Padua, the government, and industry; and (3) the RFP at the AIST Laboratory in Tsukuba, Japan. There is also a smaller experiment, EXTRAP T2R, operating in Sweden.

The combination of comparably sized poloidal and toroidal magnetic fields, plus a large aspect ratio, imply that radial pressure balance and MHD stability can be accurately modeled by a straight cylindrical system. Toroidal effects make a small quantitative modification to the results but do not qualitatively affect the overall MHD behavior.

A schematic diagram of an RFP is illustrated in Fig. 5.10. Experimentally a typical RFP operates as follows. The discharge chamber is pre-filled with neutral deuterium. Next a small, uniform toroidal bias field, which homogeneously fills the chamber, is applied by the toroidal field coils. A large toroidal current is then induced in the plasma. This is accomplished by making the torus the secondary of a transformer. As the toroidal current rises it ionizes the deuterium and compresses both the resulting plasma and the toroidal bias field. In addition the toroidal current raises the plasma temperature by ohmic heating. At the end of the current rise the peak poloidal magnetic field due to the current and the on-axis compressed toroidal bias magnetic field are of comparable size. The follow-on "flat top" portion of the current cycle is where most of the interesting MHD and confinement physics takes place.

An interesting feature of the RFP is associated with the compression of the toroidal bias field. There is substantial compression so that at the end of the

current ramp the residual edge toroidal field is much less than the central toroidal field as well as the initial bias field. Remarkably, under certain operating conditions the edge toroidal field spontaneously reverses direction, thereby motivating the name "reversed field pinch." The best performance of an RFP occurs when the field reverses. In support of this statement it is shown in Chapter 11 that without the reversal the RFP is unstable to internal MHD instabilities.

Current experimental programs are aimed at improving MHD and transport in RFPs by (1) feedback stabilizing external MHD modes, (2) external profile control, (3) operating in the single helicity state, and (4) learning how to drive long-lived toroidal currents without DC transformer action.

The analysis below considers radial pressure balance in a cylindrical RFP. The goal is to identify the critical equilibrium parameters of interest to experimental operation and to show that there is a wide range of parameter space where equilibria are possible. This range is narrowed considerably in Chapter 11 when MHD stability is analyzed.

The equilibrium p *and* B_z *profiles*

Radial pressure balance in an RFP satisfies the general screw pinch relation given by Eq. (5.20). For an RFP it is convenient to specify the pressure and toroidal field. One then uses the screw pinch pressure balance relation to determine the poloidal field.

The stability analysis in Chapter 11 shows that for internal MHD stability the pressure profile must be very flat on axis. Also, for good confinement it is desirable for the pressure and pressure gradient to vanish at the edge of the plasma $r = a$. A simple choice that captures these features is given by

$$p(\rho) = p_{\max}(1 - \rho^6)^3 \tag{5.42}$$

where $\rho = r/a$ is the normalized radius. The quantity $p_{\max}$ is the maximum pressure that occurs on axis. It is related to the average pressure by the relation

$$\langle p \rangle = 2\int_0^1 p\,\rho\,d\rho = \frac{81}{140}\,p_{\max} \tag{5.43}$$

The pressure profile $p/p_{\max}$ is illustrated in Fig. 5.11.

Consider next the $B_z(\rho)$ profile. During the flat top period of operation the toroidal field is peaked on axis and reverses direction near the plasma edge. Also, for good confinement the corresponding current density must vanish at the plasma edge. A simple form of B_z, and the corresponding J_θ, having the desired properties can be written as

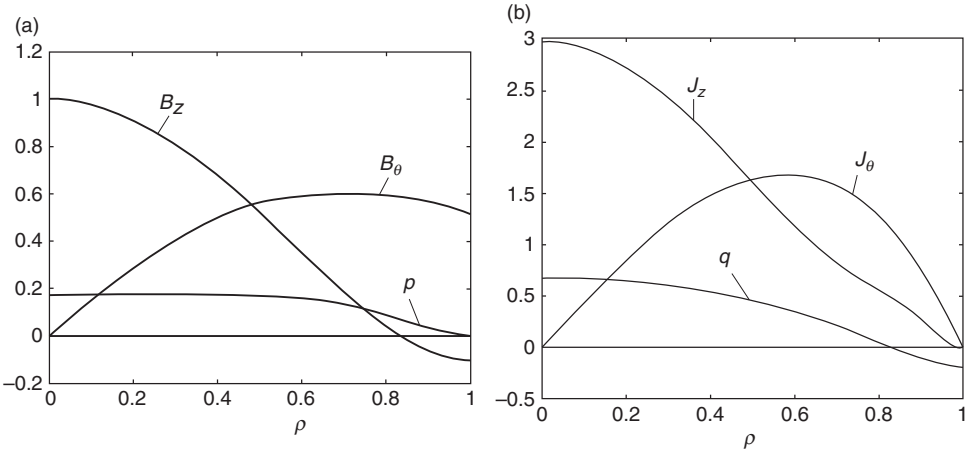

Figure 5.11 Equilibrium profiles for an RFP for the case $\alpha_z = 1.1$, $2\mu_0\langle p\rangle/B_{z0}^2 = 0.1$, and $\varepsilon = 1/5$: (a) B_z/B_{z0}, B_θ/B_{z0}, $2\mu_0 p/B_{z0}^2$ and (b), $a\mu_0 J_\theta/B_{z0}$, $a\mu_0 J_z/B_{z0}$, q/ε.

$$\frac{B_z(\rho)}{B_{z0}} = 1 - 2\alpha_z\rho^2 + \alpha_z\rho^4$$
$$\frac{a\mu_0 J_\theta(\rho)}{B_{z0}} = -\frac{1}{B_{z0}}\frac{dB_z}{d\rho} = 4\alpha_z\rho\,(1-\rho^2) \tag{5.44}$$

Here, B_{z0} is the field on axis and α_z is a parameter that measures the size of the edge toroidal field. Specifically,

$$\alpha_z = 1 - \frac{B_z(a)}{B_{z0}} = 1 - \frac{B_{za}}{B_{z0}} \tag{5.45}$$

Field reversal requires $\alpha_z > 1$. The B_z/B_{z0} and $a\mu_0 J_\theta/B_{z0}$ profiles are illustrated in Fig. 5.11 for the case $\alpha_z = 1.1$.

The B_θ *profile*

The B_θ profile is easily found from the following alternate form of the screw pinch pressure balance relation:

$$\frac{d}{d\rho}\left(\rho^2 B_\theta^2\right) = -\rho^2\frac{d}{d\rho}\left(2\mu_0 p + B_z^2\right) \tag{5.46}$$

A straightforward integration yields the somewhat complicated expression

$$\frac{B_\theta^2(\rho)}{B_{z0}^2} = \frac{\alpha_p}{9}\left(35\rho^6 - 40\rho^{12} + 14\rho^{18}\right) + \frac{\alpha_z}{15}\left[30\rho^2 - 20(2\alpha_z+1)\rho^4 + 45\alpha_z\rho^6 - 12\alpha_z\rho^8\right] \tag{5.47}$$

where $\alpha_p = 2\mu_0\langle p\rangle/B_{z0}^2$ is a parameter related to the plasma beta. The corresponding current density is found from Ampere's law

$$\frac{a\mu_0 J_z(\rho)}{B_{z0}} = \frac{1}{B_{z0}}\left[\frac{1}{\rho}\frac{d}{d\rho}(\rho B_\theta)\right] = \frac{1}{2B_{z0}}\left[\frac{1}{\rho^2 B_\theta}\frac{d}{d\rho}(\rho^2 B_\theta^2)\right]$$
$$= \frac{140\alpha_p}{9}\left(\frac{\rho B_{z0}}{B_\theta}\right)\rho^4(1-\rho^6)^2 + 4\alpha_z\left(\frac{\rho B_{z0}}{B_\theta}\right)(1-\rho^2)(1-2\alpha_z\rho^2+\alpha_z\rho^4) \tag{5.48}$$

The B_θ/B_{z0} and $a\mu_0 J_z/B_{z0}$ profiles are also illustrated in Fig. 5.14 assuming that $\alpha_p = 0.1$.

Most of the desirable RFP profile properties just described were pointed out in the early analyses of Butt *et al.* (1958), Robinson (1971), and Bodin and Newton (1980).

Figures of merit

Consider now the safety factor profile. From the definition of q it follows that

$$q(\rho) = \varepsilon\frac{\rho B_z}{B_\theta} \sim \varepsilon \ll 1 \tag{5.49}$$

where $\varepsilon = a/R_0 \ll 1$. This quantity is also plotted in Fig. 5.11 assuming that $\varepsilon = 0.2$. Observe that $q(\rho)$ decreases monotonically with radius and passes through zero at the reversal point. Particularly important is the fact that $q \sim \varepsilon$. The safety factor is small, suggesting that kink instabilities may be a problem for the RFP. For the case under consideration one finds that at the plasma edge $q_a = q_* \approx -0.039$. Stabilization requires a close fitting conducting shell and/or feedback. This conclusion is quantified in Chapter 11.

Global pressure balance

Global pressure balance in an RFP is described by a simplified form of the general screw pinch relation, obtained by making use of the fact that for typical operation, $|B_{za}| \ll B_{\theta a}$. It then follows that a useful definition of β in an RFP is given by

$$\beta = \frac{2\mu_0\langle p\rangle}{B_{za}^2 + B_{\theta a}^2} \approx \frac{2\mu_0\langle p\rangle}{B_{\theta a}^2} = \beta_p \tag{5.50}$$

The plasma is held in equilibrium primarily by the poloidal magnetic field implying that $\beta \approx \beta_p$ in an RFP.

For the present profiles β_p can be evaluated by noting that from Eq. (5.47)

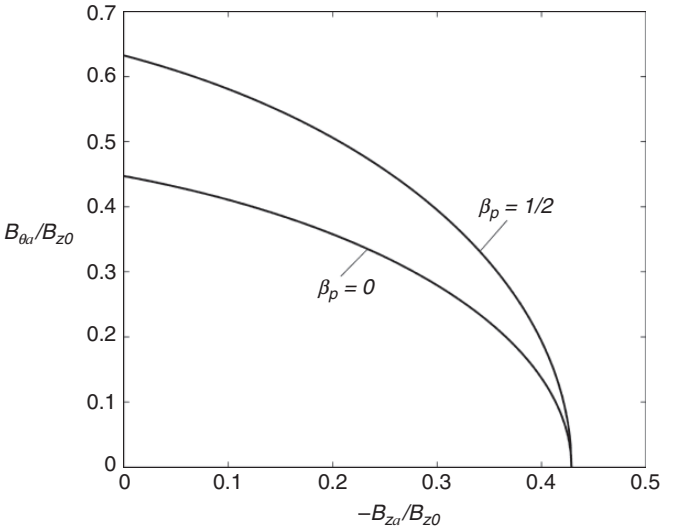

Figure 5.12 Typical operating space for an RFP in a $B_{\theta a}/B_{z0}$, B_{za}/B_{z0} diagram. The operating space lies below the curves.

$$B_{\theta a}^2 = 2\mu_0\langle p\rangle + \frac{B_{z0}^2}{15}\alpha_z(10 - 7\alpha_z) \tag{5.51}$$

leading to

$$\beta_p = \frac{15\alpha_p}{15\alpha_p + \alpha_z(10 - 7\alpha_z)} \tag{5.52}$$

The operating regime of an RFP is thus defined by the two-dimensional (α_z, α_p) parameter space with the resulting β_p given by Eq. (5.52). For the example under consideration with $\alpha_z = 1.1$ and $\alpha_p = 0.1$, one finds that $\beta_p \approx 0.37$.

The (α_z, α_p) space is equivalent to a $B_{\theta a}/B_{z0}$, B_{za}/B_{z0} space. One boundary of the latter space has already been defined: $-B_{za}/B_{z0} > 0$ for reversal. Next, the requirement that $(B_{\theta a}/B_{z0})^2 > 0$ restricts B_{za}/B_{z0} to the range $-B_{za}/B_{z0} < 3/7$. Lastly, $0 < \beta_p < 1/2$ for normal operation of an RFP. The typical operating parameter space defined by these conditions is illustrated in Fig. 5.12. Operation outside these boundaries is possible but in general corresponds to degraded performance. There are further restrictions on the operation space that arise due to MHD stability as discussed in Chapter 11.

Summary of the RFP

The RFP is a relatively large aspect ratio axisymmetric toroidal configuration with a flat pressure profile on axis and a reversed B_z near the plasma edge. The particle pressure, and toroidal and poloidal magnetic pressures are all of comparable

magnitude with the poloidal field providing the dominant force for radial pressure balance. The modest toroidal field system is a technological advantage from the reactor point of view but a sophisticated feedback system is needed to stabilize external MHD modes because of the small safety factor.

5.5.2 The low β ohmic tokamak

Overview

The tokamak is also an axisymmetric toroidal configuration. It is currently the leading contender to become the first power producing fusion reactor. Tokamaks have a large toroidal field and a small poloidal field with an aspect ratio typically on the order of $R_0/a \sim 3$. This combination of field ratio and aspect ratio leads to a safety factor satisfying $q \gtrsim 1$. The large safety factor leads to good MHD stability, even without a conducting wall or feedback, and the large toroidal field helps reduce energy and particle transport. The result is that the tokamak has exhibited the best plasma physics performance at the present time in terms of the Lawson parameter $p\tau_E$ and the ion temperature T_i as compared to all other fusion concepts. This is why it is the leading contender for a fusion reactor. However, the requirement of a large toroidal field introduces technological complexity into the configuration as well as increased capital cost.

In any event from the perspective of MHD equilibrium and stability it is worth noting that there are two qualitatively different regimes of operation of a tokamak, depending on the method of heating. The first regime corresponds to early tokamaks heated entirely by the ohmic current induced in the plasma. Here, the plasma acts as the secondary of a transformer. In this regime the plasma β is very low and the toroidal field is slightly paramagnetic. Temperatures on the order of 1–3 keV have been achieved at densities of about $10^{20}\,\mathrm{m}^{-3}$. Since the plasma resistivity decreases with increasing electron temperature (i.e., $\eta \sim T^{-3/2}$) there is a practical upper limit to how high the temperature can be raised solely by ohmic heating: $T_{\max} \sim 3$–5 keV.

With respect to stability, a low β ohmic tokamak is susceptible to MHD modes which limit the maximum toroidal current that can flow in the plasma. This corresponds to a minimum stable value of q. Violation of the current limit leads to violent MHD behavior that rapidly terminates the plasma and can in fact cause physical damage to the surrounding vacuum chamber. This catastrophic behavior is known as a "major disruption" and clearly must be avoided in a tokamak reactor. In fact many would agree that, alpha physics aside, the major plasma physics problems facing the tokamak reactor concept are the achievement of steady state and the avoidance of disruptions.

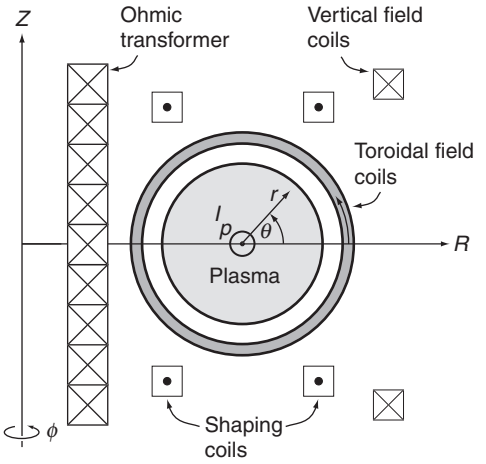

Figure 5.13 Schematic diagram of an ohmically heated tokamak with a circular cross section plasma.

Both radial pressure balance and the MHD current limit can be reasonably accurately calculated, at least for circular cross section plasmas, using the straight cylindrical model. Toroidal effects enter only as small corrections that do not affect the qualitative MHD behavior. It is the radial pressure balance of this configuration that is described in this subsection.

Before proceeding though it is worth describing the second regime of tokamak operation, which corresponds to the situation where a substantial amount of auxiliary power, provided either by neutral beams or RF waves, is injected into the plasma. This additional power raises the plasma temperature, and hence β as well. In the auxiliary heated regime toroidal effects are important, affecting both MHD equilibrium and stability. There is an equilibrium limit on βq^2 and separate stability limits on both β and q. The implication is that a high β auxiliary heated tokamak is inherently a 2-D configuration. Its equilibrium and stability properties are discussed in Chapters 6 and 12 respectively.

Return now to the low β circular tokamak. Typical operation is described in the schematic diagram illustrated in Fig. 5.13. Initially the toroidal field coils are energized, leading to a large, steady state B_z field. Neutral gas, usually deuterium, is injected into the vacuum chamber, and sometimes pre-ionized. The toroidal current is then ramped up by means of a changing flux in the primary of the ohmic transformer. After a short time, on the order of milliseconds, the plasma becomes fully ionized and achieves a steady state power balance between ohmic heating and thermal conduction losses. Radiation losses are usually small. The plasma is maintained in quasi-steady state as long the flux continues to swing at a constant rate in the primary of the transformer. This is the requirement to induce a constant

(in time) toroidal electric field in the plasma (i.e., $2\pi R_0 E_z = -d\psi/dt \approx$ constant) which drives the quasi-steady state toroidal current. Once the transformer runs out of volt-seconds the toroidal current can no longer be maintained and the plasma decays away. The time period of quasi-steady state current is known as the "flat top period" and it is here that most of the interesting physics takes place.

Note that while the current is ramping up and during flat top operation the current in the vertical field coils must be carefully programmed to hold the plasma in toroidal force balance. The shaping coils are also carefully programmed to generate the desired cross sectional shape of the plasma which was chosen as circular in the early days of fusion research, but now usually corresponds to an elongated, outward pointing "D."

Qualitatively, operation of a low β tokamak and an RFP are similar. Quantitatively though the large toroidal field in the tokamak leads to a very different flat top plasma. The large B_z field in a tokamak greatly inhibits the toroidal flux compression so that the flat top plasma is only slightly paramagnetic: $B_z(0) \approx B_z(a)$. Recall that an RFP has much more compression leading to $B_z(0) \gg B_z(a)$ and in fact $B_z(a)$ actually reverses sign.

In current high β tokamak experiments the plasma always passes through an ohmic phase before the auxiliary heating is applied. Ohmic heating is a simple way to produce a relatively high-temperature, high-density, high-quality target plasma into which auxiliary power can be efficiently injected and absorbed.

The analysis below focuses on radial pressure balance in a low β tokamak. The pressure and toroidal current profiles are determined by a simple ohmic heating power balance relation. The goal is to show that for typical experimental parameters, β will always be very low and the toroidal field will be slightly paramagnetic.

Simple transport profiles for p *and* B_θ

For a low β tokamak it is convenient to specify the $p(r)$ and $B_\theta(r)$ profiles and then use the general screw pinch pressure balance relation to determine $B_z(r)$. To specify reasonable profiles a short transport calculation is first required. Assume the torus has been straightened into a cylinder of length $2\pi R_0$ and minor radius a. The $p(r)$ and $B_\theta(r)$ profiles are determined by noting that during flat top operation power balance requires $P_\Omega = P_\kappa$: the input ohmic heating power balances the thermal conduction losses. This power balance can be expressed as

$$\frac{1}{r}\frac{d}{dr}\left(rn\chi\frac{dT}{dr}\right) + \eta J_z^2 = 0 \tag{5.53}$$

Here, it is assumed that $T_e = T_i \equiv T$. The resistivity is given by the usual Spitzer formula: $\eta = C_\eta/T^{3/2}\Omega$-m, where $C_\eta = 3.3 \times 10^{-8}$ when $T = T_k$ is measured in keV or $C_\eta = 6.7 \times 10^{-32}$ for T in joules.

The quantity χ is the thermal diffusivity which is in general anomalous and not well understood theoretically. A qualitatively correct model for the thermal diffusivity that greatly simplifies the analysis is given by $\chi = \chi_0(T_0/T)^{1/2}$, where χ_0 and T_0 are the on axis values for the diffusivity and temperature respectively. This expression takes into account that χ, as determined experimentally, is an increasing function of radius. Also, experimental data shows that $\chi_0 \gtrsim 1\,\mathrm{m}^2/\mathrm{sec}$.

The density profile is qualitatively similar to that of the temperature and is therefore chosen as $n = n_0(T/T_0)$, where n_0 is the density on axis. Lastly, the current density profile can be expressed in terms of the temperature by noting that Ohm's law requires $E_z = \eta J_z$. Furthermore, in steady state flat top operation Faraday's law implies that $\nabla \times \mathbf{E} = 0$ leading to $E_z = E_{z0} =$ constant. Thus, $J_z = E_{z0}/\eta$. In practice, the electric field is adjusted to produce a given desired current so that J_{z0} rather than E_{z0} is the parameter of experimental interest. The end result is that one can write the current density as $J_z = J_{z0}(T/T_0)^{3/2}$.

Combining these results leads to the following simplified differential equation for the quantity $U = (T/T_0)^{3/2}$ in terms of normalized radius $\rho = r/a$:

$$\begin{gathered}\frac{1}{\rho}\frac{d}{d\rho}\left(\rho\frac{dU}{d\rho}\right) + k^2 U = 0 \\ k^2 = \frac{3C_\eta a^2 J_{z0}^2}{2n_0\chi_0 T_0^{5/2}} = 0.31\left(\frac{I_M}{a\langle U\rangle}\right)^2 \frac{1}{n_{20}\chi_0 T_{k0}^{5/2}}\end{gathered} \tag{5.54}$$

where in the practical formula $I_M = I(\mathrm{MA})$, $n_{20} = n_0(10^{20}\ \mathrm{m}^{-3})$ and use has been made of the relations

$$\begin{aligned}\langle Q\rangle &= 2\int_0^1 Q\rho\, d\rho \\ I &= 2\pi\int Jr\, dr = \pi a^2 J_{z0}\langle U\rangle\end{aligned} \tag{5.55}$$

The boundary conditions on U for a confined plasma with no internal sources are given by $U'(0) = 0$ and $U(1) = 0$. Also, U has been normalized so that $U(0) = 1$. The solution is easily found and is given by

$$U = \mathrm{J}_0(k\rho) \tag{5.56}$$

where $\mathrm{J}_0(k\rho)$ is the usual Bessel function and $k = 2.405$ corresponds to the first zero. Also, it immediately follows that $\langle U\rangle = 2J_1(k)/k \approx 0.43$. Using this value for k one finds from Eq. (5.54) that the temperature on axis has the value

$$T_{k0} = 0.61\left(\frac{I_M^2}{n_{20}\chi_0 a^2}\right)^{2/5}\ \mathrm{keV} \tag{5.57}$$

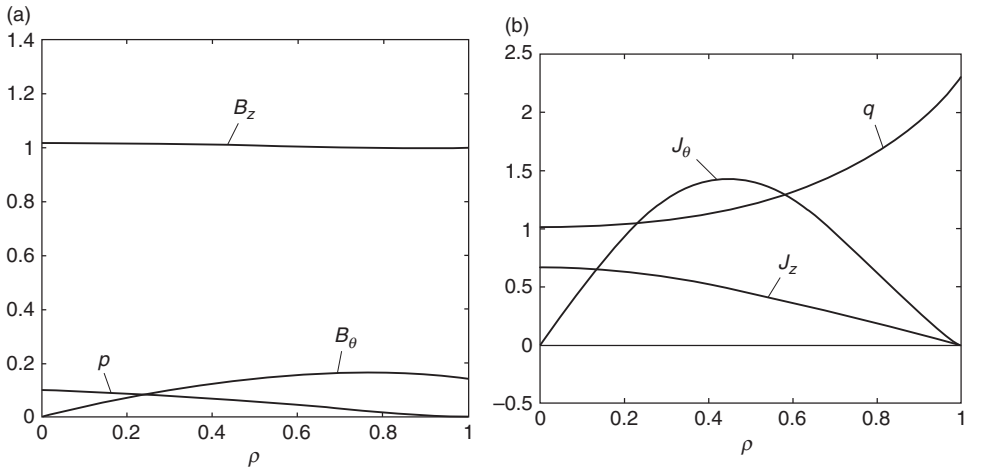

Figure 5.14 Equilibrium profiles for an ohmically heated tokamak for the case $\varepsilon = 1/3$, $q_* = 2.3$, $q_0 = 1$, and $\beta_0 = 0.002$: (a) B_θ/B_0, B_z/B_0, $(q_*/\varepsilon)^2(2\mu_0 p/B_0^2)$ and (b) $a\mu_0 J_z/B_0$, $a\mu_0 J_\theta/B_0$, q.

It is now straightforward to evaluate the desired profiles of J_z, B_θ, and p:

$$\begin{aligned}
\frac{a\mu_0 J_z(\rho)}{B_0} &= \frac{a\mu_0 J_{z0} U}{B_0} = \frac{\varepsilon}{q_*}\frac{k\mathrm{J}_0(k\rho)}{\mathrm{J}_1(k)} \\
\frac{B_\theta(\rho)}{B_0} &= \frac{\mu_0 a}{B_0 \rho}\int_0^\rho J_z\,\rho\,d\rho = \frac{\varepsilon}{q_*}\frac{\mathrm{J}_1(k\rho)}{\mathrm{J}_1(k)} \\
\frac{2\mu_0 p(\rho)}{B_0^2} &= \frac{4\mu_0 nT}{B_0^2} = \beta_0\left[\mathrm{J}_0(k\rho)\right]^{4/3}
\end{aligned} \tag{5.58}$$

Here, $B_{\theta a} = \mu_0 I/2\pi a$, $\varepsilon = a/R_0$, $q_a = q_* = \varepsilon B_0/B_{\theta a}$, $\beta_0 = 4\mu_0 n_0 T_0/B_0^2$, and B_0 is the applied toroidal field at $r = a$.

These profiles are illustrated in Fig. 5.14 for typical values $\varepsilon = 1/3$, $q_* = 2.3$, and $\beta_0 = 0.002$. Observe that both pressure and current density are monotonically decreasing functions that vanish at the plasma edge. The pressure gradient also vanishes at the edge.

The $\mathrm{B_z}$ *profile*

The remaining quantity of interest is the B_z profile which is determined by integrating the general screw pinch pressure balance relation. A short calculation yields

$$\begin{aligned}
B_z^2(\rho) &= B_0^2 - 2\mu_0 p + \mu_0 a\int_\rho^1 J_z B_\theta\,d\rho \\
&= B_0^2 - 4\mu_0 n_0 T_0 \mathrm{J}_0^{4/3}(k\rho) + \frac{B_{\theta a}^2}{2J_1^2(k)}\mathrm{J}_0^2(k\rho)
\end{aligned} \tag{5.59}$$

A good approximation to B_z is obtained by noting that in a large aspect ratio tokamak (i.e. $\varepsilon \ll 1$) the toroidal field pressure is large compared to both the poloidal field pressure and plasma pressure. In this limit

$$\frac{B_z(\rho)}{B_0} \approx 1 - \frac{\beta_0}{2} \mathrm{J}_0^{4/3}(k\rho) + \frac{\varepsilon^2}{k^2 q_0^2} \mathrm{J}_0^2(k\rho) \tag{5.60}$$

where $q_0 = 2B_0/\mu_0 R_0 J_{z0}$ is the safety factor on axis. The corresponding current density profile is given by

$$\begin{aligned} \frac{a\mu_0 J_\theta(\rho)}{B_0} &= -\frac{1}{B_0}\frac{dB_z}{d\rho} \\ &\approx \left[-\frac{2}{3} k\beta_0 \mathrm{J}_0^{1/3}(k\rho) + \frac{2\varepsilon^2}{k q_0^2} \mathrm{J}_0(k\rho) \right] \mathrm{J}_1(\rho) \end{aligned} \tag{5.61}$$

The B_z and J_θ profiles are illustrated in Fig. 5.14. Note that $B_{z0}/B_0 > 1$ implying that for the parameters chosen, the toroidal field is paramagnetic. This, as shown below, is actually a general feature of ohmic tokamaks.

Figures of merit

Having calculated the equilibrium profiles one is now in a position to evaluate the safety factor. For the ohmic tokamak model under consideration one finds

$$q(\rho) = \frac{\varepsilon \rho B_z}{B_\theta} \approx q_0 \frac{k\rho}{2\mathrm{J}_1(k\rho)} \tag{5.62}$$

The safety factor is illustrated in Fig. 5.14. Observe that q is a monotonically increasing function of the radius.

A crucial feature of tokamaks is that the toroidal magnetic field must be large enough for a given toroidal current to ensure that $q_0 \approx 1$ for favorable MHD stability. Another property of interest predicted by the model is the ratio of edge to central safety factor. Using the value $k = 2.405$ leads to

$$\frac{q_a}{q_0} = \frac{q_*}{q_0} = \frac{k}{2\mathrm{J}_1(k)} \approx 2.3 \tag{5.63}$$

This is reasonably close to typical experimental values for high-current ohmic tokamaks.

Global pressure balance

The final topic of interest is the global pressure balance. There are two points to discuss. First it is shown that in practical situations the poloidal beta in an ohmic tokamak is always less than unity, implying that the toroidal field is paramagnetic. Second, it is shown that the corresponding value of beta is always very small, thereby motivating the need for additional auxiliary heating.

The poloidal beta is defined as

$$\beta_p = \frac{2\mu_0 \langle p \rangle}{B_{\theta a}^2} \tag{5.64}$$

The expression for β_p can be written in a simple and convenient form which is a function of the actual thermal diffusivity χ_0 and the ideal classical collisional thermal diffusivity $\chi_\perp$ as follows. First, one notes that $B_{\theta a} = \mu_0 I/2\pi a$ and $\langle p \rangle = 2n_0 T_0 \langle U^{4/3} \rangle$. This yields

$$\beta_p = 16\pi^2 \langle U^{4/3} \rangle \frac{a^2 n_0 T_0}{\mu_0 I^2} = 56.8 \frac{a^2 n_0 T_0}{\mu_0 I^2} \tag{5.65}$$

The quantity $n_0 T_0$ can be rewritten by making use of the definition of k^2 given by Eq. (5.54) plus several classical transport results from Braginskii. Specifically, Eq. (5.54) can be rearranged as

$$n_0 T_0 = \left(\frac{3}{2\pi^2 k^2 \langle U \rangle^2}\right)\left(\frac{C_\eta}{T_0^{3/2}}\right)\left(\frac{I^2}{a^2 \chi_0}\right) = 0.142\left(\frac{C_\eta}{T_0^{3/2}}\right)\left(\frac{I^2}{a^2 \chi_0}\right) \tag{5.66}$$

while Braginskii has shown that

$$\begin{aligned} \eta_\parallel &= \frac{C_\eta}{T_0^{3/2}} = 0.51 \frac{m_e}{n_0 e^2 \tau_{e0}} \\ \chi_\perp &\approx \chi_i = 2^{1/2}\left(\frac{m_i}{m_e}\right)^{1/2} \frac{m_e T_0}{e^2 B_0^2 \tau_{e0}} \end{aligned} \tag{5.67}$$

Here $\eta_\parallel$ is the parallel resistivity and $\chi_\perp$ is the perpendicular thermal diffusivity (essentially due to the ions), both evaluated on axis. The electron collision time on axis τ_{e0} is now eliminated from these two quantities yielding an expression for $C_\eta/T_0^{3/2}$ as a function of $\chi_\perp$. This result is then substituted into Eq. (5.66). A short calculation leads to

$$(n_0 T_0)^2 = 0.0512\left(\frac{m_e}{m_i}\right)^{1/2}\left(\frac{I^2 B_0^2}{a^2}\right)\left(\frac{\chi_\perp}{\chi_0}\right) \tag{5.68}$$

The desired expression for β_p is obtained by substituting Eq. (5.68) into Eq. (5.65) and making use of the definition $q_* = 2\pi a^2 B_0/\mu_0 R_0 I$:

$$\beta_p \approx 2.0\left(\frac{q_*}{\varepsilon}\right)\left(\frac{m_e}{m_i}\right)^{1/4}\left(\frac{\chi_\perp}{\chi_0}\right)^{1/2} \tag{5.69}$$

For a typical ohmic tokamak $q_* \approx 2.3$ and $\varepsilon \approx 1/3$. Assuming a deuterium mass ratio one then finds

$$\beta_p \approx 1.82\left(\frac{\chi_\perp}{\chi_0}\right)^{1/2} \tag{5.70}$$

For classical transport (i.e., $\chi_0 = \chi_\perp$) then $\beta_p \approx 2$. The plasma is slightly diamagnetic. However, the actual plasma transport is highly anomalous with the smallest, most optimistic, measured value of diffusivity given by $\chi_0 \approx 1\ \mathrm{m}^2/\mathrm{sec}$. On the other hand, Braginskii gives the classical value of thermal diffusivity in Eq. (5.67) as $\chi_\perp = 0.085\, n_{20}/B_0^2 T_k^{1/2} = 1.06 \times 10^{-2}\ \mathrm{m}^2/\,\mathrm{sec}$, with the numerical value corresponding to $n_{20} = 2$, $B_0 = 4$, $T_k = 1$, and $\ln \Lambda = 19$. This yields a very small value of poloidal beta: $\beta_p \approx 0.18$. The conclusion is that without a large improvement in the thermal diffusivity an ohmic tokamak will always have $\beta_p \ll 1$. This in turn implies that the toroidal field will always be paramagnetic, which can be seen by rewriting the general screw pinch pressure balance relation given by Eq. (5.21) as follows:

$$\text{paramagnetism} \equiv \frac{1}{2B_{\theta a}^2}\int_0^1 \left(B_z^2 - B_0^2\right)\rho\, dr = 1 - \beta_p > 0 \tag{5.71}$$

Clearly for the right-hand side to be positive for a monotonic $B_z\,(\rho)$ profile requires $B_z^2(\rho) > B_0^2$. The condition $B_z^2(\rho) > B_0^2$ is the definition of toroidal paramagnetism.

The second topic of interest for global pressure balance is the value of beta. Since $B_z \gg B_\theta$ it follows that

$$\beta = \frac{2\mu_0\langle p\rangle}{B_0^2 + B_{\theta a}^2} \approx \frac{2\mu_0\langle p\rangle}{B_0^2} = \beta_t \tag{5.72}$$

The total beta is approximately equal to the toroidal beta. This quantity is always small as can be seen by eliminating $\langle p\rangle$ using the definition of β_p. One finds

$$\beta \approx \beta_t = \frac{B_{\theta a}^2}{B_0^2}\beta_p = \frac{\varepsilon^2}{q_a^2}\beta_p \tag{5.73}$$

For the model profile $\varepsilon = 1/3$, $q_a = 2.3$, and $\beta_p = 0.094$ yielding $\beta \approx 0.002$. Such small values of β are typical for ohmically heated tokamaks and are too low to be of practical use in a fusion reactor. The low value of β combined with the practical upper limit on temperature due to ohmic heating provide a strong motivation to add a substantial amount of auxiliary power to the tokamak. This leads to the high β tokamak which is inherently a 2-D configuration, discussed in Chapters 6 and 12.

Summary of the low β tokamak

The low β ohmically heated tokamak is an axisymmetric toroidal device with a large toroidal magnetic field. The plasma pressure and poloidal magnetic field are both small. The toroidal field is paramagnetic and thus does not help maintain the plasma in radial pressure balance. The main purpose of the toroidal field is to provide stability against MHD modes driven by the toroidal plasma current; that is, a large toroidal field is necessary to keep $q \gtrsim 1$. A large safety factor is one main reason why tokamak physics performance has surpassed that of other confinement concepts. However, from a technological point of view the need for a large toroidal field adds complexity and cost to a tokamak fusion reactor. Overall, the practically achievable temperatures and MHD stable beta values, while good, are still too low for a fusion reactor, thereby motivating the addition of auxiliary heating.

5.6 Summary

An examination of MHD equilibria in one-dimensional cylindrically symmetric configurations focuses attention on the problem of radial pressure balance. Toroidal force balance effects do not enter. Both toroidal and poloidal fields can provide radial pressure balance. This has been demonstrated for the limiting cases of the θ-pinch and Z-pinch, as well as for the general case of the screw pinch, the latter configuration containing an arbitrary combination of B_z and B_θ. A summary of the properties of these configurations is as follows:

- **The θ-pinch:** The θ-pinch is the one-dimensional analog of the torus with purely toroidal fields: $B_z(r)$, $J_\theta(r)$, $p(r)$. In this configuration, radial confinement is provided by the externally applied magnetic pressure. The θ-pinch is capable of a wide range of toroidal β, $0 < \beta_t < 1$. It has an infinite safety factor, $q(r) = \infty$, which is favorable for stability, although detailed calculations show that the worst modes are marginally stable.
- **The Z-pinch:** The Z-pinch is the one-dimensional analog of the torus with purely poloidal fields: $B_\theta(r)$, $J_z(r)$, $p(r)$. Here, radial pressure balance is provided by the tension in the magnetic field lines. In a Z-pinch the poloidal β is always unity: $\beta_p = 1$. The configuration has a zero safety factor, $q(r) = 0$, which is a strong indication of instability. One way to potentially avoid these instabilities is by the addition of a hard-core current-carrying wire along the axis of the device.
- **The general screw pinch:** The screw pinch is the one-dimensional analog of toroidal configurations with both toroidal and poloidal magnetic fields; for example, the low β ohmically heated tokamak and the reversed field pinch. Screw pinch configurations are capable of a wide variation in both β_t and β_p. In general, the kink safety factor q_* and the safety factor $q(r)$ are non-zero. The function $q(r)$ can increase or decrease away from the origin. For an RFP the

safety factor is small, $q \sim \varepsilon$. It decreases away from the axis and reverses near the outside of the plasma. For the low β tokamak, the safety factor is an increasing function of radius with $q_0 \sim 1$, $q_a \sim 2.5$. The implications are that RFPs should be susceptible to current-driven kink modes thereby requiring some form of feedback stabilization, while tokamaks should have more favorable stability with respect to these modes.

References

Bennett, W.H. (1934). *Phys. Rev.* **45**, 980.
Bodin, H.A.B., and Newton, A.A. (1980). *Nucl. Fusion* **20**, 1255.
Braginskii, S.I. (1965). In *Reviews of Plasma Physics*, Vol. 1, ed. M.A. Leontovich. New York: Consultants Bureau.
Butt, E.P., Curruthers, R., Mitchell, J.T.D., Pease, R.S., Thonemann, P.C., Bird, M.A., Blears, J. and Hartill E.R. (1958). In *Proceedings of the Second United Nations International Conference on the Peaceful Uses of Atomic Energy*. Geneva: United Nations, Vol. 32, p. 42.
Robinson, D.C. (1971). *Plasma Phys.*, **13**, 439.

Further reading

Below are some recent general references that specifically discuss 1-D cylindrical MHD equilibria

Bateman, G. (1978). *MHD Instabilities*. Cambridge, MA: MIT Press.
Boyd, T.J.M. and Sanderson, J.J. (2003). *The Physics of Plasmas*. Cambridge: Cambridge University Press.
Goedbloed, J.P. and Poedts, S. (2004). *Principles of Magnetohydrodynamics*. Cambridge: Cambridge University Press.
Goldston, R.J. and Rutherford, P.H. (1995). *Introduction to Plasma Physics*. Bristol: IOP Publishing Ltd.
Stacey, W.M. (2005). *Fusion Plasma Physics*. Weinheim, Germany: Wiley-VCH.

Problems

5.1 Consider a θ-pinch with a magnetic field $\mathbf{B} = B(r)\mathbf{e}_z$ and pressure $p = p(r)$. Assume $p(r) = p_0 \exp(-r^2/a^2)$, $B(\infty) = B_0$, $n(0) = 3 \times 10^{22}\,\mathrm{m}^{-3}$, $T_i(0) = 2\,\mathrm{keV}$, $T_e(0) = 0.8\,\mathrm{keV}$, $B_0 = 8T$, and $a = 0.01\,\mathrm{m}$. The temperature profiles are related to the density profile as follows: $T_i(r)/T_i(0) = T_e(r)/T_e(0) = n^2(r)/n^2(0)$.

(a) Calculate $\beta_0 \equiv \beta(0)$
(b) Draw a diagram indicating the direction of $\mathbf{B}$ and the plasma current density $\mathbf{J}$.
(c) Calculate the magnitude and sign of the curvature drift of a thermal ion and a thermal electron at $r = a$.
(d) Calculate the magnitude and sign of the ∇B drift of a thermal ion and a thermal electron at $r = a$.
(e) The signs in step (d) appear to be inconsistent with the current direction in step (b)? Explain how this inconsistency is resolved.

5.2 Consider a static ideal MHD Z-pinch equilibrium with

$$J = c_1 \frac{r^2/a^2}{(1 + r^2/a^2)^3}$$

where c_1 is a constant.

(a) Calculate $B_\theta(r)$ and $p(r)$. Express your answers in terms of I, the total current. Sketch the fields and the currents.
(b) Since $J(r)$ vanishes for large r the Z-pinch is apparently confined by its own current. Doesn't this violate the virial theorem? Explain.

5.3 In MHD equilibrium theory one often specifies $p(\psi)$ rather than $p(r)$. This problem demonstrates how the specification of $p = p(\psi)$ leads to a determination of the equilibrium fields.

(a) Consider a one-dimensional θ-pinch. Show that the flux contained within a given radius r is equal to $2\pi r A_\theta$, where A_θ is the vector potential.
(b) Define $\psi = rA_\theta$ and assume p is specified as follows: $p(\psi) = p_0 \exp(-\psi/\psi_0)$ with p_0 and ψ_0 constants. Using the one-dimensional radial pressure balance for a θ-pinch derive a differential equation for $\psi(r)$. This equation should be a first-order, non-linear differential equation. For convenience write the equation in terms of the normalized variables and parameters defined by

$$H = \psi/\psi_0 \qquad \lambda = a^2 B_0/\psi_0$$
$$x = r^2/a^2 \qquad \beta_0 = 2\mu_0 p_0/B_0^2$$

Here, B_0 is the magnetic field far from the plasma and a is a scale factor representing the characteristic plasma radius.
(c) Solve the equation for $H(x)$ subject to the condition $\psi(0) = 0$. Calculate and sketch $p(r)$ and $B_z(r)$.
(d) Calculate $\lambda = \lambda(\beta)$ by defining the scale length a such that

$$\pi p_0 a^2 = \int p(r)\, r dr d\theta$$

5.4 Prove that the safety factor on axis for a screw pinch is given by

$$q(0) = \frac{2B_z(0)}{\mu_0 R_0 J_z(0)}$$

5.5 The magnetic shear in a screw pinch is defined as

$$s(r) = \frac{r}{q}\frac{dq}{dr}$$

Assume now that the current density vanishes at the edge of the plasma: $J_z(a) = J_\theta(a) = 0$. Prove that the edge shear has the value

$$s(a) = 2$$

5.6 In tokamaks and reversed field pinches the safety factor $q(r) = rB_z/R_0B_\theta$ is an important quantity of physical interest.

(a) Assume a force-free configuration (i.e., $\nabla p = 0$) and derive a differential equation for $B_z(r)$ assuming that $q(r)$ is the known free function.
(b) Consider the $q(r)$ profile given by

$$q(r) = q_0 \frac{r_0}{(r_0^2 - r^2)^{1/2}}$$

where q_0 is the safety factor on axis and r_0 is a parameter. Find the value of r_0 as a function of the plasma edge a that makes $J_z(a) = J_\theta(a) = 0$.
(c) Calculate $\mathbf{B}(r)$ and $\mathbf{J}(r)$ assuming that $B_z(0) = B_{z0}$ and $q_0^2 = (2/3)\,\varepsilon^2$, where $\varepsilon = a/R_0$. Plot your results.

5.7 A rigid rotor θ-pinch is characterized by a current density $\mathbf{J} = J_\theta(r)\mathbf{e}_\theta$ that is related to the number density by $J_\theta(r) = -e\Omega rn(r)$, where $\Omega = \text{const}$. Assume for simplicity that the temperature and density are related by $T(r) = T_0n(r)/n_0$, where T_0 and n_0 are the on-axis values.

(a) Derive the differential equation that determines $n(r)$.
(b) Determine $n(r)$ assuming that $n(a) = 0$.

5.8 Consider a constant pitch screw pinch defined by the requirement that $B_\theta(r) = krB_z(r)$, where k = constant. Assume that the pressure is given by $p = p_0(1 - r^2 / a^2)^2$.

(a) Calculate $B_z(r)$
(b) Show that there is no choice of k and p_0 that leads to $J_\theta(a) = 0$. The current can never vanish at the edge of a constant pitch screw pinch with confined pressure.

5.9 This problem investigates the use of "gravity" in a slab geometry to model plasma rotation and magnetic field line curvature.

(a) Derive the one-dimensional radial pressure balance relation for a general screw pinch including the effect of a stationary angular velocity $\Omega(r)\mathbf{e}_\theta$.
(b) Derive the one-dimensional pressure balance relation for a slab model of a plasma including a gravity $g(x)\mathbf{e}_x$. Assume $\rho(x)$, $p(x)$, $B_y(x)$, and $B_z(x)$ are non-zero. Also assume there is no equilibrium flow: $\mathbf{v} = 0$.

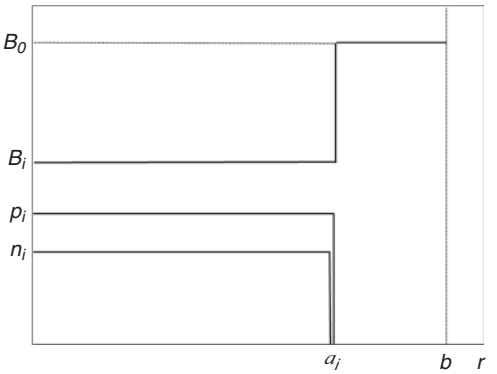

Figure 5.15 Surface current model of a θ-pinch.

(c) By comparing the results in (a) and (b) determine a correspondence between B_θ, Ω, and g so that gravity models the effects of rotation and poloidal field line tension.

5.10 This problem treats the adiabatic compression of a θ-pinch. Consider the simple surface current model of an infinitely long, straight θ-pinch as shown in Fig. 5.15. Here, n_i, p_i, B_i, a_i, and B_0 represent the initial known state of the plasma. At $t = 0$, the applied field at $r = b$ is slowly (i.e., adiabatically) increased until B_0 reaches the value $B_0' = \lambda B_0$. The quantity $\lambda > 1$ is the multiplication factor of the applied field and is assumed known. Also, the plasma obeys an adiabatic equation of state.

(a) Derive, but do not solve, an algebraic equation which relates the final β of the plasma (β_f) to the initial beta of the plasma (β_i). Express this equation in the form $F(\beta_f, \beta_i, \lambda, \gamma) = 0$, where γ is the ratio of specific heats.
(b) Solve this equation analytically for the special case $\gamma = 1$, $\beta_i = 0.5$, and $\lambda = 2$.
(c) Solve this equation numerically for the special case $\gamma = 5/3$, $\beta_i = 0.5$, and $\lambda = 2$.
(d) If you did the problem correctly you should find that $\beta_f < \beta_i$ for both cases. Explain why the final β decreases even though the plasma has been compressed.

5.11 An early description of a low β screw pinch is provided by the "force-free paramagnetic" model. In this model one sets $\nabla p = 0$ and assumes a resistive Ohm's law $\mathbf{E} + \mathbf{v} \times \mathbf{B} = \eta \mathbf{J}$. In steady state $\mathbf{E} = E_0 \mathbf{e}_z$.

(a) Use the pressure balance relation and the parallel component of Ohm's law to derive a coupled set of differential equations for $B_z(r)$ and $B_\theta(r)$.

(b) Solve these equations (numerically) assuming that η = constant. Assume the minor radius of the plasma is $a = 0.3\,\mathrm{m}$ and the current density on axis is $J_z(0) = 1\,\mathrm{MA/m^2}$.

5.12 Magnetic profile measurements on a straight screw pinch indicate that the B_θ profile is given by

$$B_\theta(r) = \frac{\mu_0 I}{2\pi}\frac{r}{r^2 + r_0^2}$$

where I is the plasma current and r_0 is the characteristic radius of the plasma. For simplicity assume that p and B_z are related by

$$B_z^2(r) = B_0^2 - 2\mu_0\lambda p(r)$$

Here, B_0 is the externally applied field and λ is a constant to be determined. Diamagnetic loop measurements indicate that the "excluded flux" has the value

$$\Delta\psi = 0.02\left(\pi r_0^2 B_0\right)$$

The "excluded flux" represents the difference between the toroidal flux contained within the conducting wall (of radius $a \gg r_0$) for the case of no plasma present and the case where plasma is present assuming the same value of B_0:

$$\Delta\psi = \psi_{tor}(\text{no plasma present}) - \psi_{tor}(\text{plasma present})$$

(a) Calculate λ. To simplify the analysis assume:

$$\mu_0 I/2\pi r_0 B_0 = 0.2 \ll 1.$$

(b) Calculate the toroidal beta if $a/r_0 = 3$.

5.13 In Section 5.5.2 it was shown that for practical situations an ohmically heated tokamak is paramagnetic with respect to the toroidal field. The goal of this problem, which makes use of the analysis in Section 5.5.2, is to determine the amount of auxiliary power required to transition the plasma from paramagnetic to diamagnetic. To carry out the analysis assume that auxiliary heating is applied to the plasma which is much greater in magnitude than the ohmic power. Specifically, replace the ohmic heating power with the auxiliary power in Eq. (5.53): $\eta J_z^2 \rightarrow S_{\mathrm{aux}}(r)$. Next, assume that the auxiliary power deposition profile is peaked on axis, which for mathematical simplicity can be modeled as $S_{\mathrm{aux}}(r) = S_0(T/T_0)^{3/2}$.

(a) Make use of the analytic results in Section 5.5.2 to find $U(r) = (T/T_0)^{3/2}$.

(b) Note that S_0 has the units of W/m^2. Derive an expression for S_0 in terms of the total power P_T and the geometry.

(c) Show that the temperature on axis is given by

$$T_0 = \left(\frac{3}{8\pi^2 k \mathrm{J}_1(k)}\right)\left(\frac{P_T}{R_0 n_0 \chi_0}\right)$$

(d) Show that the poloidal beta in the plasma is given by

$$\beta_p = \left(\frac{6\langle U^{4/3}\rangle}{\mu_0 k \mathrm{J}_1(k)}\right)\left(\frac{a^2 P_T}{I^2 R_0 \chi_0}\right) = 0.36\left(\frac{6}{\mu_0 k \mathrm{J}_1(k)}\right)\left(\frac{a^2 P_T}{I^2 R_0 \chi_0}\right)$$

(e) Calculate the value of P_T at the transition point for diamagnetism using typical parameters for TFTR: $R_0 = 2.4\,\mathrm{m}$, $a = 0.8\,\mathrm{m}$, $I = 1.2\,\mathrm{MA}$, $\chi_0 = 1\,\mathrm{m}^2/\mathrm{sec}$, and $n_0 = 0.5 \times 10^{20}\,\mathrm{m}^{-3}$. Calculate the corresponding value of T_{k0}.